

High electrical conductivity in nonlinear model lattice crystals mediated by thermal excitation of solectrons

Alexander P. Chetverikov^{1,2}, Werner Ebeling^{1,3}, Gerd Röpke^{1,4}, and Manuel G. Velarde^{1,a}

¹ Instituto Pluridisciplinar, Universidad Complutense, Paseo Juan XXIII, 1, 28040 Madrid, Spain

² Departement of Physics, Saratov State University, Astrakhanskaya 83, 410012 Saratov, Russia

³ Institut für Physik, Humboldt Universität Berlin, Newtonstrasse 15, 12489 Berlin, Germany

⁴ Institut für Physik, Universität Rostock, Universitätsplatz 2, 18055 Rostock, Germany

Received 27 March 2014 / Received in final form 2 June 2014

Published online 14 July 2014 – © EDP Sciences, Società Italiana di Fisica, Springer-Verlag 2014

Abstract. The quantum statistics of electrons interacting with nonlinear excitations of a classical heated nonlinear lattice of atoms is studied. By using tight-binding approximation, Wigner momentum distributions and computer simulations we show the existence of quite fast and nearly loss-free motions of charges along crystallographic axes and estimate the range of values of transport coefficients. Using minimization of free energy we estimate the density of mobile bound states between electrons and lattice solitons (so-called solectrons). We calculate the momenta of Wigner velocity distributions and from Kubo relations the diffusivity and the electrical conductivity using the relaxation time approximation. We show that thermally excited solectrons in nonlinear media may lead to a significant transport enhancement. Our estimates and computer simulations demonstrate the existence of a temperature window, where solectrons are relatively stable and contribute strongly to transport. The electrical conductivity may be enhanced up to two orders of magnitude.

1 Introduction

Examples of nonlinear lattices conducting electricity are, e.g., doped polymers like trans-polyacetylene (tPA) which are already used in many present-day technologies [1–3]. Their underlying theory is based upon the so-called SSH Hamiltonian proposed by Su et al. [4]. Related models of interest for our purpose in this work, using the tight-binding approximation (TBA), were provided by Holstein [5,6], Davydov [7–9] and others [10–16]. Here, we are dealing with the influence of lattice anharmonicity and lattice solitons on electric transport having also in mind conducting polymers, biomolecules, and other materials like graphene [17] and carbon nanotubes [18]. The high conductivity of carbon nano-tubes and graphene nano-ribbons seems to correspond to ballistic conduction [18]. However, further insight seems needed to really assess the foundations of the process. We also feel that the arguments we develop in the present work may have also some relevance for the understanding of the conducting stripes in cuprate materials which are observed in high-temperature-superconductors [19,20].

Our basic idea is that thermal solitons may be excited along atomic lattices and mostly traveling along crystal-

lographic axes, which would be responsible of high enhancement of electron transport. Let us recall that the electrical current, j , depends on the number density of the charges, n , the charge itself, e , and the drift velocity, v_d , or mobility, μ ,

$$j = nev_d, \quad v_d = \langle v \rangle = \mu E.$$

In the linear (Ohmic) case, the conductivity is given by $\sigma = ne\mu$. In general, mobilities are given in $\text{cm}^2/\text{V s}$, with typical values like $\mu < 10$ for amorphous Si and for standard organic semiconductors, $\mu \sim 10^3$ for silicon at room temperature, and $\mu \simeq 2 \times 10^5$ for graphene, at low temperature, and for conducting polymers such as polydiacetylene (PDA), etc. at room temperature.

At variance with earlier approaches we here concentrate on soliton-assisted transport which goes beyond the common phonon-assisted transport. We do this by generalizing the earlier mentioned model Hamiltonians [4–16] taking into account the effect of anharmonic excitations like lattice solitons capable of binding charges. The Holstein model for a weakly coupled quantum system of (spinless) electrons and phonons has been studied extensively as paradigmatic quantum-mechanical model for polaron formation in systems with dominant short-range electron-lattice interactions. The closely related Davydov model [7,8], later extended by Scott [10,11] and others, is a

^a e-mail: mgvelarde@pluri.ucm.es

mixed classical-quantum model and was originally developed for applications to proteins and other biopolymers. The approach in the present work also builds upon some of our earlier work [21–25], but now focusing on the influence of temperature on transport properties. A result we already found is that there is a range of “optimal” temperatures where the conductivity may be enhanced by about two orders of magnitude due to the influence of lattice solitons. In order to get high conductivities we need either high density of charges like in metals, high velocity of the charges (as in Tokamaks and polymer materials), or high charge as in dusty plasma. Standard good conductors like Cu and Ag, have high conductivity due to their high density of the degenerate electrons in the conduction band. Standard superconductors have also high electron density but high-temperature superconductivity appears not necessarily connected with high densities. High conductivity in materials with low density of itinerant electrons is observed in conducting polymers as in polyenes (polyacetylen, polydiacetylene, etc.). To our knowledge the values of electrical conductivity of doped polyacetylene are in the range 10^4 – 10^6 S m $^{-1}$, with the highest value reported so far, for stretched oriented polyacetylene, is 8×10^6 S m $^{-1}$. Some thirty years ago, in PDA crystals and derivatives, drift velocities, v_d , up to 5 km/s were observed experimentally by Donovan and coworkers [26–28] which could be attributed to the assistance provided by lattice solitons [29–32].

Solitons are indeed at the core of tPA electric transport [1]. Noteworthy is that lattice solitons and solertrons (bound states of electrons to solitons) exhibit supersonic velocity [31], in the range of a few km/s for parameter values of most of the materials mentioned above. Here we estimate the number density and the momentum distributions of thermally excited solertrons in order to show that they may contribute to reach high values of conductivity and other related transport properties.

We will consider thermal systems with temperatures in the range $T \simeq 10^1$ – 10^2 K. We estimate the density of solertrons by mass-action methods, estimate Wigner momentum distributions analytically and from computer simulations to calculate transport properties from non-Maxwellian bimodal distributions.

2 The tight-binding Hamiltonian for the electron lattice dynamics

As noted above, the Hamiltonian proposed by Davydov [7,8] and by Su et al. [4] is of mixed classical quantum type. For one-dimensional model lattice crystals with atoms coupled by Morse forces, in which one excess electron has been added, we use a generalization of such Hamiltonian. Thus we take

$$H = H_{lat} + H_{edi} + H_{end}. \quad (1)$$

Here H_{lat} accounts for the classical dynamics of longitudinal (acoustic) relative vibrations of the atoms along the lattice to be specified below. The TBA Hamiltonian

is given by its diagonal, H_{edi} , and off-diagonal, H_{end} , contributions

$$H_{edi} = \sum_n E_n c_n c_n^\dagger, \quad (2)$$

$$H_{end} = - \sum_n V_{n,n-1} (c_n^\dagger c_{n-1} + c_{n-1}^\dagger c_n). \quad (3)$$

The index n denotes the site of the n th atom along the lattice. In occupation number representation (so mis-called second quantization) the $|c_n|^2$ determine the probability to find the electron (charge) residing at the site n . We define the shifts of the site positions from the initial rest state, $z_n^0 = na$, by $u_n = z_n - na$. Here a denotes the atomic distance at equilibrium. The energy E_n and the transition integrals $V_{n,n-1}$ may depend on the position of the sites to the linear approximation we have:

$$E_n(u_i) = E_n^0 + \chi [(u_{n+1} - u_n) + (u_n - u_{n-1})].$$

Davydov called exciton or polaron contribution the part of the Hamiltonian depending just on E_n . Here χ accounts for an interaction term which describes the polarization effects. Both terms give rise to nonlinearities. For simplicity here we neglect onsite terms, thus ruling out the Holstein Hamiltonian [5,6]. For materials mentioned above, the polarization constant is of the order $\chi \simeq 0.1$ – 0.2 eV/Å. Depending on the strength of these terms we may observe the formation of Landau-Pekar polarons [33,34] or excitons or Davydov-Scott solitons. The Landau-Pekar polaron is a bound state of an electron to the local electrical polarization deformation of the lattice, pinned or mobile, with an effective mass exceeding the mass of the free electron. Solitary solutions corresponding to stronger interactions than the one considered by Pekar were first studied by Davydov [8]. A different mechanism for creating soliton-like phenomena is connected with the off-diagonal terms $V_{n,n-1}$. The latter transfer matrix elements, or transition integrals (otherwise called nearest neighbor electron interaction energy), have values determined by nearest-neighbor overlap integrals being responsible for the hoppings of the electron along the lattice. Following Slater [35] we assume an exponential dependence:

$$V_{n,n-1} = V_0 \exp[-\alpha(u_n - u_{n-1})], \quad (4)$$

where $u_n = z_n - na$ are as before the elongations from rest positions. The quantity V_0 often denoted by letter J in Davydov’s notation or t_0 in conducting polymers theory delineates the hopping strength. As (4) shows that the $V_{n,n-1}$ depend on the relative elongations of two nearest neighbors along the lattice. The quantity α regulates how strongly $V_{n,n-1}$ is influenced by the distance. When $\alpha = 0$, $\chi = 0$, i.e., when the coupling between electrons and the lattice is absent, the electron dynamics is independent from the lattice and is described by a discrete Schrödinger equation for the electron wave function components c_n . The effective mass of the free motion is related to the transfer integral by $m_{\text{eff}} = \hbar^2/2Ja^2$. We note that the eigenfunctions are periodic functions and so all

processes are periodic. The eigen energies have the band structure typical for lattice systems.

The case $\alpha = 0, \chi > 0$ was analyzed in detail by Davydov, Scott and others. A rather complete mathematical and numerical analysis of this Hamiltonian was also given by Zolotaryuk et al. [13]. It has been shown, that the originally subsonic selftrapping Davydov-Scott polaron-like mode in a nonlinear lattice with cubic nonlinearity bifurcates beyond the sound velocity in at least three ways. One of them is supersonic still like the selftrapping mode of the Davydov-Scott soliton. The other two are intimately coupled to the anharmonicity of the lattice and hence bear some similarity with the starting concept in the present work.

By linearization of the transition integral (Eq. (4)), we get a contribution $V_0\alpha(u_{n-1} - u_n)$ which constitutes one of the non-linearities in the SSH-theory [1,4] like originally in the Landau-Pekar polaron approach. In practice, this electron-phonon interaction Hamiltonian with a zero polarization term $\chi = 0$ is used for modeling the hopping of the π -electrons in polyenes and their interaction with lattice deformations. The SSH-Hamiltonian describes topological (kink) soliton-like excitations [4]. A detailed analysis of the different effects due to the terms χ and α [25] has shown that the strength of the nonlinear effects generated by the diagonal term χ and those by the off-diagonal term α are of the same order, provided the values of both quantities are similar $\chi \sim \alpha$. Besides, solitons due to off-diagonal effects appear beyond a certain critical value of the electron-lattice coupling αV_0 .

For the lattice part of the Hamiltonian, H_{lat} , describing relative longitudinal changes of the equilibrium positions of the atoms we assume Morse potentials [36]. The Hamiltonian is then:

$$H_{lat} = \sum_n \left\{ \frac{p_n^2}{2m_0} + D(1 - \exp[-b(u_n - u_{n-1})])^2 \right\}. \quad (5)$$

Note that in 2d- or 3d-lattices a crystallographic axis permits defining a quasi-one-dimensional sublattice dynamics. D is the break-up energy of a bond, b is the stiffness parameter of the potential and m_0 denotes the mass of atoms (all having equal mass). The Morse potential exhibits an exponential-repulsive part preventing the cross-over of neighboring lattice atoms for large displacements. Note that, with a Taylor expansion of the exponential function in equation (5) one recovers in lowest order the harmonic limit and in next order one recovers the cubic anharmonic potential. With the addition of the anharmonic lattice, universality of the description is achieved by introducing new scales. Time, t , is then made dimensionless as: $\tilde{t} = \omega_0 t$, with $\omega_0 = \sqrt{2Db^2/m_0}$ being the frequency of harmonic oscillations around the minimum of the Morse potential. The energy of the electrons is measured in units of $\hbar\omega_0$. The dimensionless remaining variables and parameters of the system are

$$q_n = b u_n, \quad V = \frac{V_0}{2D}, \quad \tilde{\alpha} = \frac{\alpha}{b}, \quad \tilde{\chi} = \frac{\chi}{b}. \quad (6)$$

The equations of motion derived from the Hamiltonian given by equations (3)–(5) are, assuming $E_n^0 = 0$,

$$i \frac{dc_n}{d\tilde{t}} = -\tilde{\chi}(q_{n+1} - q_{n-1})c_n - \tau \left[\exp[-\tilde{\alpha}(q_{n+1} - q_n)]c_{n+1} + \exp[-\tilde{\alpha}(q_n - q_{n-1})]c_{n-1} \right], \quad (7)$$

$$\frac{d^2 q_n}{d\tilde{t}^2} = [1 - \exp\{-(q_{n+1} - q_n)\}] \exp[-(q_{n+1} - q_n)] - [1 - \exp\{-(q_n - q_{n-1})\}] \exp[-(q_n - q_{n-1})] - \tilde{\alpha}V \{ (c_{n+1}^*c_n + c_{n+1}c_n^*) \exp[-\tilde{\alpha}(q_{n+1} - q_n)] - (c_n^*c_{n-1} + c_n c_{n-1}^*) \exp[-\tilde{\alpha}(q_n - q_{n-1})] \}. \quad (8)$$

The adiabaticity parameter $\tau = V_0/(\hbar\omega_0)$, appearing in the r.h.s. of equation (7) determines the degree of time scale separation between the (fast, ultraviolet) electronic and (slow, infrared) acoustic processes. For illustration we use the following values: $\tau = 10$, $V = 0.1$, and $\tilde{\alpha} = 1.75$ which are significant, e.g., for hydrogen bonded biomolecules [7,8,10,23]. For conducting polymers the range of $\tilde{\alpha} = 0.5-1.75$ seems appropriate. Note that in what follows we may drop the tilde, if misunderstanding is excluded.

As shown by Su et al. [4] there are kink-like states breaking the left-right symmetry of the system. This leads to a degeneration of the ground state of the system. As shown in [25], the kinks and corresponding localized electronic states appear only at supercritical values of the electron-lattice coupling $\alpha > \alpha_{cr} \simeq (1/4\sqrt{V})$. Let us discuss now the continuum approximation of the discrete dynamic equations (7) and (8). To simplify we take into account only weak nonlinearities by including only the first higher correction to the harmonic case. Linearizing the Morse interaction potential we find

$$V_M(r) = -D + \frac{k_0}{2}(r-a)^2 + \frac{\gamma_0}{3}(r-a)^3, \quad (9)$$

with $k_0 = 2Db^2$ denoting the linear (Hooke) elasticity constant and $\gamma_0 = 3Db^3$ accounts for (weak) anharmonicity. The oscillation time is typically in the picosecond range $\omega_0 \sim 10^{12}-10^{13} \text{ s}^{-1}$. In the dimensionless quantities introduced before typical sets of values are $ba \sim 1-4$, $\gamma_0 \sim 3-9$, $\tilde{\chi} \sim 0.2$, $\tilde{\alpha} \sim 1-2$. Needless to say, the systematic linearization of all nonlinearities in our Hamiltonian (3)–(5) leads to the SSH-Hamiltonian [4], including the cubic term proportional to γ_0 leads to the SSH Hamiltonian [4]. Further, the case $\alpha = 0$ leads to the Davydov Hamiltonian [8]. For not too strong nonlinearities, continuum approximations allow analytical estimates. We can transform equations (7) and (8) to partial differential equations for the envelope of the wave function and the compression

deformation density, respectively [8,13]:

$$i\hbar\phi_t + \frac{\hbar^2}{2m}\phi_{zz} + g\rho\phi = 0, \quad (10)$$

$$\rho_{tt} - k_0\rho_{zz} + \gamma_0(\rho^2)_{zz} - \frac{a^2}{12}\rho_{zzzz} + g(\phi^2)_{zz} = 0. \quad (11)$$

The compression deformation density $\rho(z, t)$ is the limit of $\rho_n = z_n - z_{n-1} - a$ and evolves according to the Boussinesq equation (11) [37]. The wave function amplitude $\phi(z, t)$ is the limit of the amplitude $c_n(t)$. Noteworthy is that with the above given approximations the nonlinearity in the electron-lattice coupling appears as:

$$g = \chi + \alpha V_0.$$

The term $(-g\rho)$ plays the role of an external potential in the Schrödinger equation for ϕ (10). Note that the validity of the continuum approximation is restricted to small values of α, χ, γ_0 .

The system modeled by the Davydov and SSH Hamiltonian [4,7] corresponding to (10) and (11) has two limit cases:

- (i) The regime of SSH topological solitons which is characterized by nearly pinned topological soliton fronts/kinks between two opposite deformation states (left/right elongation from the rest states). This regime is akin to polaron effect limited to the parameter interval $1 < \tilde{\alpha} < 2$ and γ_0 small or even zero [25].
- (ii) The regime of lattice solitons is characterized by rather energetic lattice solitons which are only weakly disturbed by the electrons. It is the genuine solectron regime for parameter values $1 \leq \tilde{\alpha} \leq 2$ and moderate γ_0 . For semiquantitative estimates, using the above indicated approximation we shall restrict consideration to the second case.

Another remark is appropriate: the electrons influence lattice oscillations of electronic bound states (exciton-polaron effects) and the electrons that influence lattice effects on transitions between sites, are not necessarily identical. Those electrons introduced by doping are strongly affected by polarization effects and shifts of bound states. On the other hand the electrons in polymers responsible for hopping, the π -electrons are strongly affected by the transition effects. If both types of electrons are described by a different basis, we might have to introduce extra creation and annihilation operators. In the simplest case we may assume that the doping electrons influence only the bound states and the π -electrons influence only the hopping transitions.

3 Solectrons-bound states between electrons and solitons

Let us now add an excess electron to the anharmonic lattice and investigate its bound state to a lattice soliton. For the one-dimensional case several analytical results for the problem of supersonic charge transfer were

obtained by Davydov and collaborators. These results are obtained only for the Davydov-Scott Hamiltonian, i.e., for $\chi > 0, \alpha = 0$. According to the results obtained in [25] we may expect that the nonlinear terms described by the parameter α act in a similar way.

The results obtained in [8,12,13] for the case of a cubic nonlinearity of the lattice are simplified in the following. With nonlinearities included, there exist two branches of solutions for the wave functions and the deformation functions. We represent the wave functions by a phase factor and an envelope function [8,38]

$$\Psi(z, t) = \exp(i(kz - \omega t))\phi(\xi), \quad (12)$$

where $\xi = z - v_{se}t$ is a coordinate running with the solectron velocity v_{se} . Let us consider now the envelope functions and the corresponding compression functions in the continuum approximation (Eqs. (10) and (11)):

- (i) The first type of soliton solutions are polaron-type solutions or Davydov-Scott-type solutions with the shape

$$\rho(\xi) \sim \text{sech}^2(\kappa\xi); \quad (\phi(\xi))^2 \sim (v_0^2 - v_{se}^2)\rho(\xi) + \gamma_0\rho^2(\xi), \quad (13)$$

where $v_0 = \omega_0 a$ is the sound velocity.

- (ii) The second type of soliton solutions are determined by the lattice nonlinearities and are called lattice polaron (lp) solutions or Davydov-Zolotaryuk solutions with the shape

$$\rho \sim \text{sech}^2(\kappa\xi); \quad (\phi(\xi))^2 \sim \rho^2(\xi), \quad (14)$$

which not being the most general ansatz it is a useful one for our purpose here. The essential differences are the relations between wave functions and deformation compression densities. Another difference is their corresponding velocities. The Davydov-Scott solutions are subsonic, but as shown in [13], they may have also a supersonic branch. On the other hand the Davydov-Zolotaryuk lp-solitons are always supersonic. However as shown in several computer experiments with discrete lattices, this evidently is an artefact of the continuum approach. If supersonic lattice solitons are “loaded” with an electron, their velocity is affected and often it goes down to values below the sound velocity. Therefore, strictly speaking, the classification into supersonic and subsonic solectrons does not have a precise meaning [31]. In the following we consider Davydov-Zolotaryuk -type solectrons with appropriate corrections- in order to extend their range of validity to the subsonic case. This can be achieved by assuming that the general solution is the addition of both types of soliton solutions. Then we make the following ansatz for the charge probability density:

$$(\phi(\xi))^2 = c_1\rho + c_2\rho^2. \quad (15)$$

Because of the normalization condition only one of these constants is free and may be used to monitor computer simulations. By introducing the ansatz (15) into the Boussinesq equation (11) we get the following modified Boussinesq equation for solitons which differs from

the original one only by renormalized coefficients

$$\rho_{tt} - (k_0 - gc_1)\rho_{zz} + (\gamma_0 - gc_2)(\rho^2)_{zz} - \frac{1}{12}\rho_{zzzz} = 0. \quad (16)$$

The result is, that in the approximation used here the compression density keeps its general shape except that the soliton velocity v_s is lowered since the lattice constant is reduced and the effective stiffness is also diminished. This corresponds to the gauge transformation:

$$k_0 \rightarrow k_1 = k_0 - gc_1, \quad \gamma_0 \rightarrow \gamma_1 = \gamma_0 - gc_2, \quad (17)$$

$$v_s^2 \rightarrow v_{se}^2 = v_s^2 - gc_1, \quad (18)$$

where g is the electron-lattice parameter coupling introduced above and v_{se} appears as the velocity of the compound electron-soliton (solectron) now of lower value than the soliton velocity. Accordingly, for the one-soliton solution

$$\rho(z, \kappa, t) \simeq \frac{k_1 \kappa^2}{2\gamma_1} \text{sech}^2(\kappa[(z(t) - z(0) \pm v_{se}t)]). \quad (19)$$

Here the parameters k_0 and γ_0 of the original Morse system are replaced by k_1, γ_1 . This corresponds to a modification of the Morse potential which is softened to a lower frequency with a weaker stiffness. This might be an oversimplification, but it agrees well with the trend seen in the computer experiments [31].

For instance, a nearly linear dependence of velocity on the electron-lattice coupling parameter V_0 was found (in particular no divergence found at $v_{se} \rightarrow v_0$). The results for the solectron velocity versus the compound electron lattice coupling parameter, αV , may be described by the relationship

$$v_{se}^2 \simeq v_s^2 - 1.8\tilde{\alpha}Vv_0^2. \quad (20)$$

A linear, albeit empirical fit may also account for the computer data points. Having in mind also quasi-one-dimensional lattices like solitons moving along crystallographic axes in a two-dimensional lattice we now consider z for a generic rectilinear axis.

Now we need the charge density of electrons $\rho_e(z, t)$ which is according to the above closely related to the compression density $\rho(z, t)$. The compression density created by solitons induces a moving polarization potential well $W(z, t) = -g\rho$, which may attract electrons and form rather stable electron-lattice bound states (Fig. 1). According to the continuum theory introduced above, the potential well creating a solectron is proportional to the lattice compression deformation density

$$W(z, \kappa, t) = -g\rho(z, \kappa, t) = -3g\frac{k_1\kappa^2a^2}{2\gamma_1}\text{sech}^2(\kappa\xi). \quad (21)$$

By means of a Galilean boost and limiting ourselves to the harmonic approximation (21) reduces to:

$$W(z, \kappa, t) \simeq g\frac{k_1\kappa^2a^2}{2\gamma_1}(-1 + \kappa^2\xi^2 + \dots), \quad (22)$$

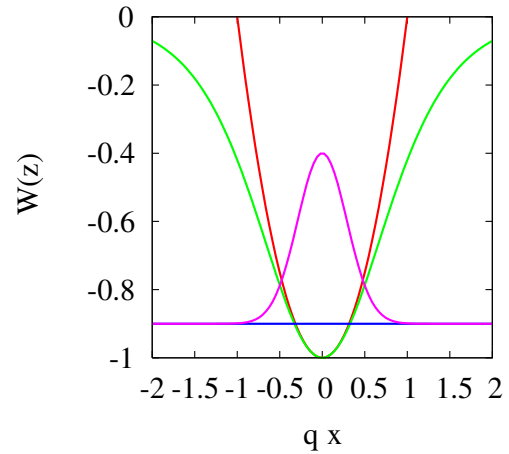


Fig. 1. The potential created by a supersonic soliton which acts on added, excess electrons in the harmonic approximation. We sketch also the ground state energy level and the shape of the wave function also in harmonic approximation.

with $\xi = z - z_0 - v_{se}t$. Note that the spring constant k_1 and the nonlinearity γ_1 are not the original ones for the Morse potential but are already renormalized quantities as explained above. We may write the harmonic approximation in another standard form

$$W(z, \kappa, t) = W_0 + \frac{1}{2}m_{se}\omega_{se}^2\xi^2, \quad (23)$$

with

$$W_0 = -g\frac{k_1\kappa^2a^2}{2\gamma_1}; \quad \omega_{se}^2 = g\frac{k_1\kappa^4a^2}{2\gamma_1}. \quad (24)$$

To further simplify the problem we recall that from the oscillator quantum mechanics the bell-shaped oscillator wave function can be written as:

$$\phi_0(\xi, t) \simeq \frac{1}{[2\pi\xi_0^2]^{1/4}} \exp\left[-\frac{\xi^2}{4\xi_0^2}\right], \quad (25)$$

$$\xi_0^2 = \langle \xi^2 \rangle = \frac{\hbar}{2m_{se}\omega_{se}}. \quad (26)$$

Recall that m_{se} is the effective mass of the “solectron” quasi-particle and ω_{se} its characteristic oscillation frequency around the minimum of the soliton well. We note that these two quantities determine most properties of the solectron system. The energy of our mobile ground state is in harmonic approximation [38]

$$E_{se} \simeq -g\frac{k_1\kappa^2a^2}{2\gamma_1} + \frac{1}{2}\hbar\omega_{se}. \quad (27)$$

This is a ground state for fixed (inverse) width κ tantamount to fixed value of the solectron velocity v_{se} . Note that this ground state is degenerated and the energies are the same for right and left running solectrons. The ground state energy is proportional to the solectron (inverse) width square, i.e., approximately to the difference between the solectron velocity square and the sound velocity square [25].

4 Thermal distributions of solitons and thermodynamic equilibria

In heated systems, low-energetic solitons will be created depending on temperature with some probability according to the canonical weights corresponding to the energy of solitons. These thermal solitons which are spontaneously formed are indeed able to trap electrons. Let us first study the number density or fraction of solitons in a heated Morse lattice. For Toda systems this problem has been studied by several authors [11,14,39–41]. The distribution with respect to the energy and the corresponding (inverse) width κ was estimated by Marchesoni and Lucheroni [41]. For Toda systems these authors showed that the density of thermal solitons, in a first approximation, goes as $T^{1/3}$. For Morse systems, following closely the approach proposed in [41] we find the fraction of lattice sites which are occupied by solitons

$$x_s^0(T) = \frac{N_s}{N} \simeq A_1[T^{1/3} - A_2T^{2/3} + O(T)], \quad (28)$$

with $A_1 \simeq 0.754$, $A_2 \simeq 1.89$. Based on the fact that the highest number of solitons is the number of lattice sites, N , we can replace (28) by a Padé approximation [21]

$$x_s^0(T) = \frac{N_s}{N} \simeq \frac{A_1T^{1/3} + BT}{1 + A_2T^{1/3} + BT}. \quad (29)$$

The value of $B = 5$ was estimated fitting results from earlier computer experiments [40,41].

The next problem is to estimate, how many of the thermal solitons are occupied by electrons, for a doping fraction d . At low temperatures we have $x_s^0 < d$ and, consequently, nearly all electrons will find a partner for forming a soliton. For simplicity, we can assume the Davydov relation between charge density and lattice compression density,

$$\rho_e(z, t) \sim \rho(z, t). \quad (30)$$

In order to estimate the number density of solitons and the corresponding number density of solitons we solved first the discrete dynamics of solitons and solitons which is determined by the dynamical equations (7) and (8). In order to visualize the charge densities several methods were developed. We have to calculate in the discrete case the distribution of

$$\rho_n(t) = q_n(t) - q_{n-1}(t). \quad (31)$$

In first approximation we may neglect quantum effects in equation (8), hence setting $\alpha V = 0$, and using classical trajectories subject to thermal noise. This method seems well suited to estimate the soliton density, the soliton number and related parameters at different temperatures. In the Langevin approach we perform computer simulations of the equation (8) with an added standard stochastic source. Examples are shown in Figure 2. At low temperatures we may identify phonon-like excitations. With increasing T soliton-like excitations appear as diagonal lines which are destroyed at too high T . In spite of the rather qualitative character of these visualizations we are able to identify several significant features:

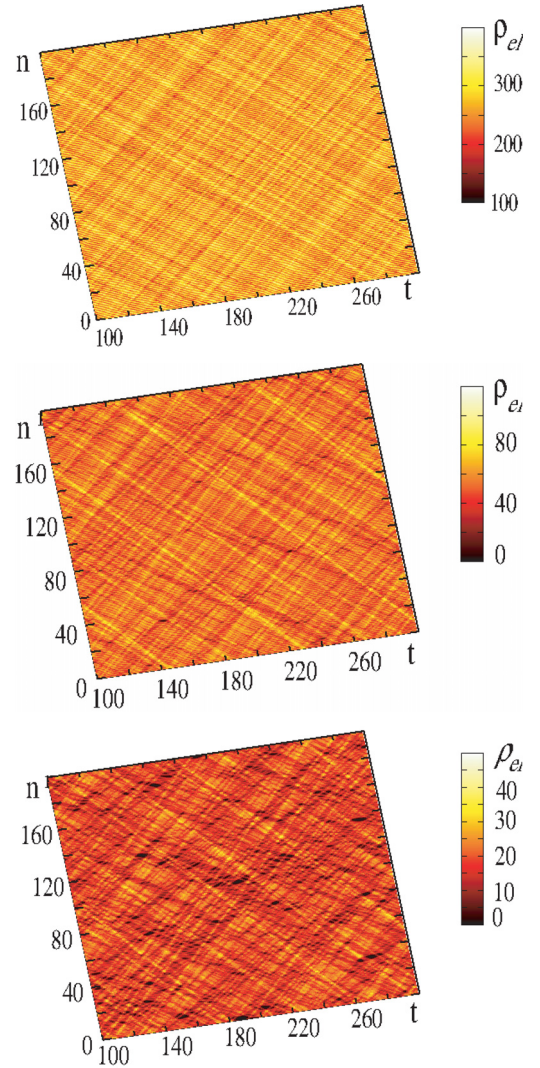


Fig. 2. Space-time trajectories (ordinate-abscissa) of solitons moving to the right or to the left for three values of the dimensionless temperature: $T = 0.01, 0.05, 0.15$.

- (i) The density of soliton-like excitations depends indeed on the temperature. It seems to have an optimum in the range of, say, moderately high temperatures. This comes from estimating the number of maxima going, at fixed time, along the interval of sites.
- (ii) Most trajectories of the soliton excitations are parallel and oriented with nearly 45 degree angle (or -45 with respect to the vertical, hence 135 degrees). This clearly means that the velocities have two preferred values left to right around the sound velocity. This follows from the slopes (the 45 degree directions) of the solitonic “stripes” in Figure 2.

We can quantify these two features by calculating the mean fraction of solitons and solitons on a lattice and subsequently their velocity or momentum distribution.

So far we tacitly assumed that all thermally excited solitons are forming solitons. This however will be violated in the region of “high” temperatures where $x_s^0 > d$.

Then the number of solitons will be lower than the number of thermal solitons. Here the doping d fraction corresponds to the relative occupation x_e^0 which is the ratio of the number of electrons (free or bound) to the total number of lattice sites $x_e^0 = d = N_e/N$. In thermodynamics this quantity is the mole fraction. In order to estimate the thermal densities of the solitons and solotrons at different temperatures and doping densities, we have to study the thermodynamic equilibria for the formation of solotrons (bisolotrons are not considered here). Note that within our highly simplified model, the electrons are always associated to one of the sites. In real systems the doping expressed as mole fraction x_e^0 may vary only within certain limits. In general it will not exceed the value 0.3–0.5, i.e., not more than 30–50 percent of lattice sites can be occupied by electrons. Let us denote the number of solotrons by N_{se}^* , their density in the lattice by $n_{se} = N_{se}^*/(Na)$ (recall that a is the lattice spacing) and the fraction by $x_{se} = N_{se}^*/N$. In first approximation [22] we may assume that the number of solotrons N_{se}^* and the number of free solitons $N_s^* - N_{se}^*$ are related by a Boltzmann factor. However this approximation has the disadvantage that the fractions may violate sometimes the condition that the solottron number cannot exceed the total number of added excess electrons. In order to maintain bounds like $N_{se}^* < N_e$ and $N_s^* < N_s$ we start here from a minimization of the free energy supplemented by the corresponding balance equations. The thermodynamic equilibrium, at fixed temperature, corresponds to the minimal free energy. This minimum depends on energy and entropy and so the free energy of thermal systems. We will use here the approximation of ideal solutions developed by Planck. In this approximation we consider the system as a mixture of the species i which has the free energy

$$F = \sum_i N_i [E_i + k_B T (\ln(N_i A_i / V) - 1)]. \quad (32)$$

The corresponding chemical potential and the thermal de Broglie wave length are given by:

$$\mu_i = E_i + k_B T \log(N_i A_i / V); \quad \Lambda_i = \frac{h}{(2\pi m_i k_B T)^{1/2}}. \quad (33)$$

In chemical equilibrium, minimizing the free energy demands that any change of the free energy due to an infinitesimal redistribution (change) of the particle numbers must vanish. This means that for a particle change the chemical potentials before and after the transitions should be equal. The corresponding equations for the chemical potentials will be derived now. Our system is a mixture of N_e^* free electrons, N_s^* free solitons and N_{se}^* solotrons. The equilibrium condition for the chemical potentials of free solitons, free electrons and solotrons, supplemented by the balance equations are:

$$\mu_s + \mu_e = \mu_{se}; \quad N_e^* + N_{se}^* = N_e; \quad N_s^* + N_{se}^* = N_s. \quad (34)$$

Using a semi-classical approximation we get

$$\mu_e = k_B T \ln \Lambda_e n_e^*; \quad \mu_s = k_B T \ln \Lambda_s n_s; \quad (35)$$

$$\mu_{se} = E_{se} + k_B T \ln \Lambda_{se} n_{se}; \quad \Lambda_i = \sqrt{2\pi} \frac{h}{\sqrt{m_i k_B T}}. \quad (36)$$

We introduce now the relative occupations by free electrons and by free solotrons (recalling that N is the total number of lattice sites).

$$x_e = \frac{N_e^*}{N}; \quad x_{se} = \frac{N_{se}^*}{N} = x_e^0 - x_e. \quad (37)$$

The coupled system may be transformed to the quadratic form

$$x_e^0 = x[1 + K_2(x_s^0 - x_e^0)] + K_2 x^2, \quad (38)$$

$$K_2(T) = \left(\frac{T_d}{T}\right)^{d/2} \exp\left(\frac{|E_{se}|}{k_B T}\right). \quad (39)$$

The solution for $x = x_e$ is easily found and we get for the relative occupation by solotrons

$$x_{se} = x_e^0 + \frac{1}{2K_2} \left[\left(1 + 2K_2 x_s^0 + 2K_2 x_e^0 + K_2^2 (x_s^0 - x_e^0)^2\right)^{1/2} - 1 - K_2 x_s^0 - K_2 x_e^0 \right], \quad (40)$$

where $x_s^0 = x_s^0(T)$ is given by equation (28). Beware that here d denotes dimension (in our case $d = 1$). Further T_d defines a degeneration temperature for the case of full occupation with electrons corresponding to number densities of about $2 \times 10^7 \text{ cm}^{-3}$. For reasonable assumptions about the masses we find values of $T_d \simeq 10^2 \text{ K}$; in units of $2D$ this is $T_d \simeq 10^{-1}$. Following Davydov, for the binding energy of the solottron, we take $|E_{se}| \simeq 0.1 \text{ eV}$ and with $D \simeq 0.1 \text{ eV}$ we get the dimensionless estimate $|E_{se}| \simeq 0.5$. Note that all these numbers are rough approximations, since the binding energies and masses are not accurately known. Two curves for the solottron fractions at doping fraction $d = 0.3$ and $d = 0.5$ as a function of the temperature are shown in Figure 3. For the calculation, we use the binding energy $|E_{se}| \simeq D$. The upper (green) curve corresponds to a doping of 50 percent and the lower curve to a doping of 30 percent. Note that the minimization of the free energy together with the correct balance of charges gives smaller fractions of solotrons and a saturation of the solottron fraction at the doping densities $x_e^0 = 0.3$ and $x_e^0 = 0.5$, respectively, as requested. We observe that the existence of solotrons on one-dimensional Morse lattices is, for realistic values of the binding energy, rather concentrated in the temperature range $T \simeq 0.05 - 0.2$. For higher temperatures the potential well of the soliton is not able to bind electrons due to energetic and entropic influences. Noteworthy is the appearance of two opposite trends. The density of thermal solitons increases with T but their ability to bind free electrons decreases with T . Accordingly, an optimal temperature range exists.

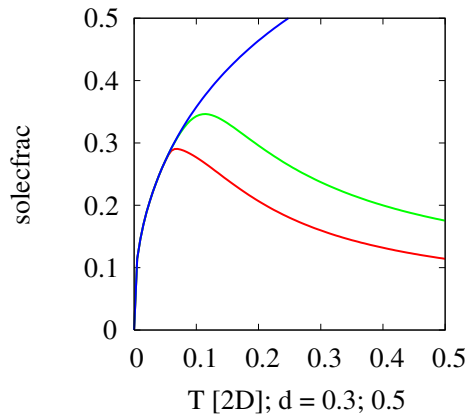


Fig. 3. Soliton and solectron fractions versus temperature T (in units $2D$) for two doping fractions N_e/N . The solectron fraction is obtained by minimization of the free energy (equilibrium of chemical potentials). The binding energy used is $|E_{se}| \simeq D$. The upper curve (green) corresponds to a doping of 50 percent and the lower curve to a doping of 30 percent. Clearly, there is kind of an optimal temperature for solectron formation around $T \sim 0.1$ (in units of $2D$).

Of particular interest is the maximum which is near to the temperature where the number of solitons $x_s(T_m)$ equals the number of electrons introduced by doping $d = x_e^0$. For a doping $d = 0.3$ this temperature is around $T_m \simeq 0.05$ and we see from Figure 3 that, indeed, nearly all doping electrons found a soliton to form a bound state. However at $d \simeq 0.5$ the effectivity in forming solectrons deteriorates. We may conclude therefore that a doping in the range $d = 0.2$ – 0.4 is somehow optimal with respect to formation of solectron bound states. Further we may conclude that solectron based applications should operate near to the optimal temperature. At temperatures beyond the maximum the soliton is no more able to bind the electron.

5 Calculation of solectron momentum distributions

Let us first further examine the computer simulations of solectron excitations shown in Figure 2. Most of the space-time trajectories have a slope of nearly ± 45 degrees, relative to the vertical, thus corresponding to unit velocity which is the sound velocity in our dimensionless units. The dispersion around the maxima of the velocities is rather small. It is compatible with the assumption of a bistable thermal distribution (around ± 45 degrees). This result purely classical is also the outcome of the integration of the mixed classical-quantum system (7) and (8) [23]. The solectrons are able to travel over distances of a few hundred lattice sites. Similar results have also been obtained at “moderately” high temperatures using Pauli master equations for the electron motion [42–44]. Here we restrict consideration to rather low to moderate temperatures solving (7) and (8) with an electron Hamiltonian

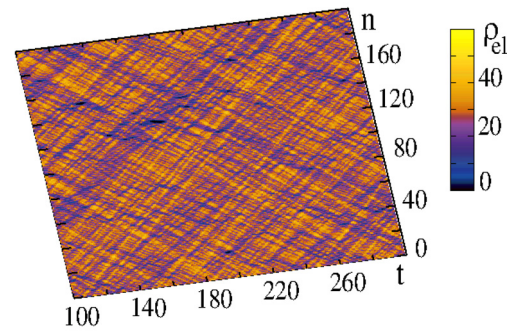


Fig. 4. Space-time trajectories of the added, excess electron probability density obtained from the integration of equations (7) and (8). Parameter values: $T = 0.1$, $ba = 1$, $\tilde{\alpha} = 1.75$, $\tau = 10$, $N = 200$.

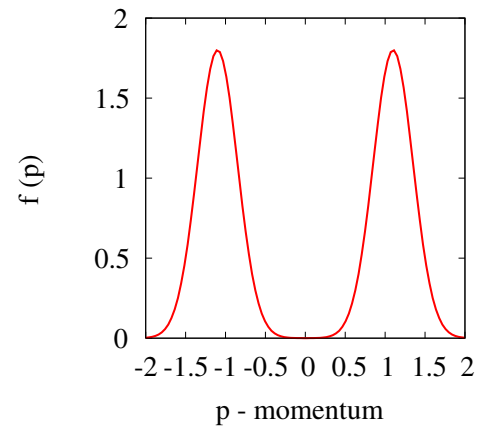


Fig. 5. Momentum distributions for $T = 0.1$ obtained from trajectories displayed in Figure 4. Parameter values: $T = 0.1$, $ba = 1$, $\tilde{\alpha} = 1.75$, $\tau = 10$, $N = 200$.

with distance-dependent transition probabilities [23]. Figure 4 illustrates the results found in one typical case, with $x_n(t)/a$ the time-dependent coordinate of the lattice atom number n in the direction of the one-dimensional motion. In qualitative agreement with Figure 2 the diagonal stripes correspond to regions of enhanced density of electrons which are freely running along the lattice, this indicates existence of solectron excitations. Checking the slopes we see that the excitations which survive more than ten time units move with *supersonic* velocity. The pictures shown are quite similar to others earlier described in the literature [14], where life-times of about two picoseconds with stability up to 10 K have been reported. In our computer simulations life-times of about 10–50 time units can be seen. Thus our solectrons survive for several picoseconds up to $T = 0.1$ which is about physiological temperatures. This confirms an earlier finding were at $T \sim 300$ K stable solitons and solectrons could be identified [23,43,44]. Purely classical computer simulations described in [39] as well as estimates based on the pseudopotential described above also show typical Gaussian stochastic trajectories with bimodal distributions as illustrated in Figure 5.

In order to derive analytical expressions let us first study the case of very low temperatures. We start from

the ground state wave function in Gaussian approximation as done above and get for a right- or left-running solitrons

$$\Psi_0(z, t) = \exp(i(kz - \omega t)\phi(\xi)), \quad (41)$$

$$\phi(\xi) = \frac{1}{[2\pi\xi_0^2]^{1/4}} \exp\left[-\frac{(x \pm v_{se}t)^2}{4\xi_0^2}\right]. \quad (42)$$

The wave function in momentum space follows by Fourier transform. It is also a Gaussian centered around the solitron momenta $p_{se} = \pm m_{se}v_{se}$,

$$\Phi_0^\pm(p_z, t) \simeq c_\pm \exp\left[-\frac{(p_z \pm m_{se}v_{se})^2}{2m_{se}\hbar\omega_{se}}\right]. \quad (43)$$

Taking w_+ and w_- as relative weights for the left and right-running excitations, respectively, the global density in momentum space is:

$$\rho_{se}(p_z, t) \simeq \frac{w_+}{\sqrt{\pi m_{se}\hbar\omega_{se}}} \exp\left[-\frac{(p_z - m_{se}v_{se})^2}{m_{se}\hbar\omega_{se}}\right] + \frac{w_-}{\sqrt{\pi m_{se}\hbar\omega_{se}}} \exp\left[-\frac{(p_z + m_{se}v_{se})^2}{m_{se}\hbar\omega_{se}}\right], \quad (44)$$

which is the sum of two Gaussian profiles. Needless to say this is just an approximation which is strictly valid only when the two wave functions do not overlap. Since overlapping occurs just during a short time interval, the approximation (44) in the thermal case appears justified. The common width of the profiles of the ground state distribution is $\hbar\omega_{se}/2$. For systems in a heat bath at finite temperature, the ‘‘effective temperature of the ground state’’, is the so-called quantum temperature. For parabolic potentials, the calculations are easily performed in the framework of Wigner functions [45–47]. The Wigner momentum distribution for a particle in an oscillator potential at rest is:

$$f(p_z) = \frac{1}{\sqrt{2\pi m k_B T_q}} \exp\left[-\frac{p_z^2}{2m k_B T_q}\right]; \quad (45)$$

$$T_q = \frac{\hbar\omega_{se}}{2k_B} \coth \frac{\hbar\omega_{se}}{2k_B T}, \quad (46)$$

with the quantum temperature T_q which, as said above, replaces the classical temperature T . We have the limits

$$T_q \rightarrow T \quad \text{if} \quad T \rightarrow \infty, \quad (47)$$

$$k_B T_q \rightarrow \hbar\omega_{se}/2 \quad \text{if} \quad T \rightarrow 0. \quad (48)$$

In other words, (45) and (46) embrace the classical as well as the quantum-mechanical case, including the ground state. Note that such a simple formula is valid only in the harmonic oscillator approximation. If, however, we use (45) and (46) for solitrons, the momenta have to be shifted and centered around the soliton velocities. As we have shown, the thermal soliton velocities have also a distribution in momentum space. In order to simplify we use, for a given temperature, instead of the thermal distribution of soliton velocities its most probable value, as

for $T < 0.5$ the distributions are rather narrow. Then we set

$$v_s^2(T) \simeq v_0^2[1 + 1.19T^{2/3}]; \quad v_{se}^2(T) \simeq v_{se}^2[1 + 1.19T^{2/3}].$$

Thus the momentum Wigner function for solitrons, in thermal equilibrium with a Morse lattice, is:

$$f_0(p_z) = \frac{w_+}{\sqrt{2\pi m k_B T_q}} \exp\left[-\frac{(p_z - m_{se}v_{se}(T))^2}{2m k_B T_q}\right] + \frac{w_-}{\sqrt{2\pi m k_B T_q}} \exp\left[-\frac{(p_z + m_{se}v_{se}(T))^2}{2m k_B T_q}\right]. \quad (49)$$

We see that the momentum Wigner function of the solitrons is bistable and looks very much like the quantum-mechanical density in the ground state (44). Our result is a rough albeit useful first-order approximation. We note further that through Tq , the frequency ω_{se} of solitron oscillations in a soliton well is a significant physical quantity in the problem.

Note that the solitron velocity v_{se} is in general much higher than the Drude velocity of electrons under low and moderate values of the electrical field, E . It is also higher than the thermal velocity. In thermal equilibrium the solitrons are no more one-sided but are equally distributed between left and right directions of motion. Then the fluctuations of solitrons are very large, since the solitrons may have positive and negative sound velocities, i.e., according to their direction of motion, what leads to electrical current fluctuations of order $e^2 v_{se}(T)^2$. Indeed, in thermal equilibrium the mean square velocity is:

$$\langle v^2 \rangle = \frac{1}{N} \int_{-\infty}^{+\infty} dp_z (p_z/m_{se})^2 \left[\exp\left(-\beta_q (p_z - p_{se})^2\right) + \exp\left(-\beta_q (p_z + p_{se})^2\right) \right], \quad (50)$$

with

$$N = \int_{-\infty}^{+\infty} dp_z \left[\exp\left(-\beta_q (p_z - p_{se})^2\right) + \exp\left(-\beta_q (p_z + p_{se})^2\right) \right], \quad (51)$$

with $\beta_q = 1/2m_{se}k_B T_q$. Carrying out the integration, (50) gives a generalized Nyquist formula for solitrons,

$$\langle v^2 \rangle = \frac{k_B T_q}{m_{se}} + v_{se}(T)^2. \quad (52)$$

The mean square velocity is the sum of a thermal part and a solitron part. The former is strongly temperature-dependent while the latter one depends only weakly on temperature and it is, in general, the dominant contribution. Note that (52) is for supersonic as well as for slightly subsonic cases. These large fluctuations are, according to the Taylor-Kubo theory, related to transport [46,48]. This appears as the physical reason for the significant enhancement of transport which we shall estimate now.

6 Enhancement of transport assisted by solitons

The dispersion of the velocities is connected with transport by the fluctuation-dissipation theorem [22,46,48]. We start with the simplest case, which is diffusion, and study the influence of solitons and, consequently, on solitons on diffusion. In the relaxation time approximation, with ν_{se} as the effective Drude-Lorentz frequency scale, the diffusion coefficient is directly proportional to the dispersion of the velocity

$$D_{se} = \frac{1}{\nu_{se}} \langle v^2 \rangle \simeq \frac{1}{\nu_{se}} \left[\frac{k_B T_q}{m_{se}} + v_{se}^2 \right], \quad (53)$$

which shows two terms, a thermal contribution called D_{th} , and a genuine solectronic contribution. When the latter dominates we can estimate the enhancement by the ratio

$$\frac{D_{se}}{D_{th}} = 1 + \frac{m_{se} v_{se}^2}{k_B T_q}. \quad (54)$$

In order to check the validity of (54) we followed numerically the temperature dependence of the mean square displacement of solitons by starting a soliton at $t = 0$ and computing the dispersion of its density. The problem reduces to solving equations (7) and (8) in their extended Langevin-Schrödinger form, hence in a thermal bath. First we heat the system to a given temperature (e.g. $T = 0.1$ in units $2D$ as in the case shown in Fig. 6). Then we add an excess electron, with electron probability density concentrated in the center of the lattice. After thermalization at temperature T the heat bath is switched-off and the dynamical system (7) and (8) is integrated using, for simplicity, a Dirac delta-like initial electron density. For not too low temperatures the computer simulations show stochastic diffusion-like trajectories. With increasing temperature the widening of the diffusive cone decreases. The spreading of the electron density permits to define a mean square displacement. Thermal solitons create a diffusion channel which stabilizes the electron dispersion. We compare in Figure 6 the points obtained from the mean square displacement with the theoretical estimate for the enhancement given by (54). The parameter values for the computer simulation are: $N = 400$, $ba = 1$, $\tilde{\alpha} = 1.75$, $\tau = 10$, and $0.01 < T < 1$. In the region of temperatures $T \sim 0.1-0.5$ the agreement is acceptable. The larger deviations at smaller and at higher temperatures may be connected with the fact that at very low T , as well as at very high T , the spreading is no more diffusion-like and the mean-square displacement cannot be obtained with enough accuracy.

Consequently, the solectronic contribution to the velocity dispersion clearly leads to an enhancement ratio proportional to the solectron velocity squared. This shows that the ratio between the solectron-driven current (or soliton-assisted transport) and the Drude current for simple electrons may be very high. It has a maximum for $T \rightarrow 0$ as seen in Figure 6. Assuming, as in earlier

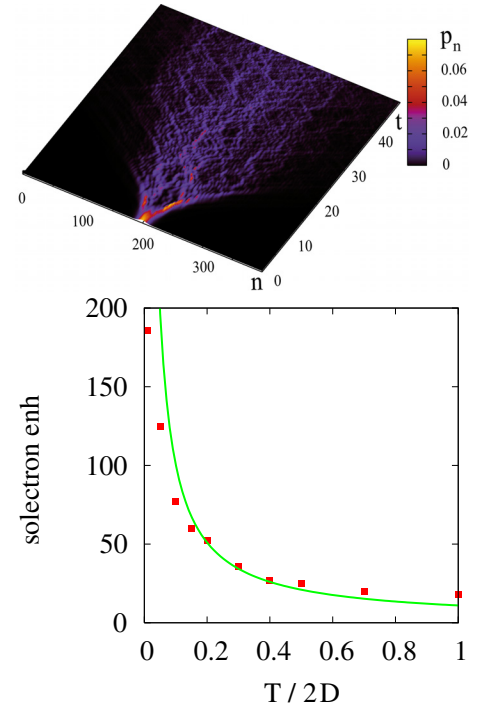


Fig. 6. Solitons in a Morse lattice. Panel above: spreading of the electron probability density for the temperature $T = 0.1$ from computer simulations with corresponding Langevin-Schrödinger equations using equations (7) and (8). Panel below: dots come from the computer simulations compared with the theoretical estimate (continuous line) obtained from equation (54) with $\tilde{a} \simeq 10^{-2}$; $\tilde{b} \simeq 10^3$ (for definitions, see main text).

work [38], for a one-dimensional lattice:

$$\begin{aligned} \omega_{se} &\simeq (10^{12}-10^{13}) \text{ s}^{-1}; & m_{se} &\simeq (1-10) m_e, \\ v_{se} &\simeq (1-2) \times 10^3 \text{ m/s}, \end{aligned}$$

we get characteristic enhancement parameters. The two most relevant are

$$\tilde{a} = \frac{\hbar \omega_{se}}{4D} \simeq 10^{-2}; \quad \tilde{b} = \frac{2m_{se} v_{se}^2}{\hbar \omega_{se}} \simeq 10^1-10^3. \quad (55)$$

Accordingly, the maximum of the enhancement factor is around the value of \tilde{b} (see Fig. 3). At low temperatures the enhancement ratio is strongly influenced by the frequency of the quantum-mechanical solectron oscillations in the potential wells created by solitons.

Let us now estimate the soliton-assisted enhancement of the electrical conductance. The fluctuation-dissipation theorem in the classical version [48] yields the electrical current as:

$$j_e = \frac{E}{k_B T} \int_0^\infty d\tau \langle j_e j_e(\tau) \rangle. \quad (56)$$

Its generalization to quantum oscillators with frequency ω_{se} is [46,48]

$$j_e = \frac{(2/\hbar \omega_{se})E}{k_B \coth(\hbar \omega_{se}/2k_B T)} \int_0^\infty d\tau \langle \hat{j}_e \hat{j}_e(\tau) \rangle. \quad (57)$$

The equilibrium distribution of a solectron is the above given Gaussian approximation and the dispersion is given by the quantum temperature. As already said the solectron velocity v_{se} is, in general, much higher than the thermal velocity and the Drude velocity of electrons. The problem of conductivity leads us back to the problem of calculating the dispersion $\langle v^2 \rangle$. The expression for the low-enough field contribution to the electrical conductivity is:

$$\sigma_{se} = \frac{n_e e^2}{k_B T_q \nu_{se}} \langle v^2 \rangle \simeq \frac{n_e e^2}{m_{se} \nu_{se}} \left[1 + \frac{m_{se} v_{se}^2}{k_B T_q} \right]. \quad (58)$$

Here we have a contribution proportional to the thermal velocities and a contribution proportional to the solectron velocities, as expected.

7 The temperature range for significant enhancement of the electrical mobility and conductivity

Let us study the mobility in electrical field which correspond to the mobility in the presence of a gradient of the electron concentration. In view of equation (58) the low-enough field contribution to the mobility of solectrons is:

$$\mu_{se} = \frac{e^2}{k_B T_q \nu_{se}} \langle v^2 \rangle \simeq \frac{e^2}{m_{se} \nu_{se}} \left[1 + \frac{m_{se} v_{se}^2}{k_B T_q} \right], \quad (59)$$

which shows the enhancement relative to the free electron case.

Here we tacitly assumed that the solectron is moving in a harmonic well and has the corresponding quantum temperature T_q . In order to characterize the difference between the mobility of an electron and solectrons we also introduce as above an enhancement ratio

$$r_1(T, v_{se}) = \frac{\mu_{se}}{\mu_e} = \left[1 + \frac{m_{se} v_{se}^2}{k_B T_q} \right] \frac{m_e \nu_e}{m_{se} \nu_{se}}. \quad (60)$$

This ratio shows, for a single solectron, how much the transport is enhanced by solectron effects relative to the Drude-Lorentz theory. Our kinetic approach fits well with the quantum kinetic theory of polaron-mediated conduction developed by Gogolin [24]. The current may also be calculated for higher fields, as shown by Gogolin [29] (see also [49]). Ultrahigh mobilities as well as the saturation effect with the increasing field strength were observed for PDA polymer crystals and derivatives some thirty years ago by Donovan and Wilson [26–28]. Here we consider only the case of low-enough field values, i.e., the linear approximation in E .

The enhancement ratio shows a strong maximum at low temperatures. Note that the singularity T^{-1} in the transport quantities observed in classical theories is ruled out by the Bose factor, which leads to a finite value of the effective temperature T_q^{-1} at zero temperature. This is a quantum cut-off proportional to \hbar . Apparently, the

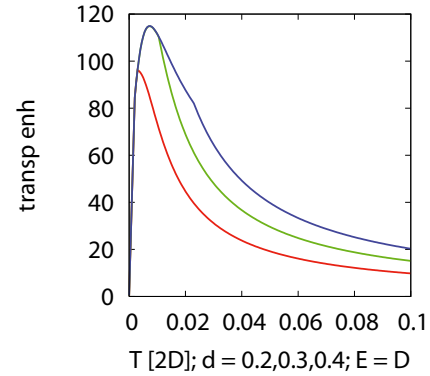


Fig. 7. Average enhancement by formation of solectrons in a Morse lattice with 20 percent (bottom red curve), 30 percent (middle green curve) and with 40 percent (upper blue curve) doping.

solectron effects increases at low temperature. This is expected to be correct since the appearance of solectrons demands adding the thermal bath to the dynamical equations. Solectrons may be formed only in the presence of thermal solitons which occur only at finite temperature. At higher temperatures a maximum of enhancement is seen and then the effect decays to zero. In our case the maximum of the effect is around $T \simeq 0.002$ in units of $2D$. The existence of such a temperature range, limited from below and above, was found already as a result of classical computer simulations [39], with however a lower enhancement factor and an optimal temperature much higher. Here the quantum corrections connected with the Bose factor [45,46] not only give much higher values for the enhancement in comparison to [39] but also shift the maximum to lower temperatures. Taking into account that such estimates were based on entirely different methods using the dynamic structure factor, such a qualitative agreement is remarkable.

Last but not least we calculate the mean enhancement of electric transport by charges in the presence of many electrons $N_e \gg 1$ and many solectrons $N_{se} \gg 1$ due to doping. Taking into account the equilibrium between solectrons (bound electrons) and free electrons, the formula (60) has to be modified since the enhancement refers only to the solectrons and not to the free electrons, which serve as reference level. Taking into account that we have the fractions x_e of free electrons and x_{se} of solectrons, the mean enhancement of specific electric transport (i.e. per unit volume or per lattice site) is:

$$\langle r_{et}(T) \rangle = x_e + r_1(T) x_{se}. \quad (61)$$

Introducing here their corresponding expressions we find

$$\langle r_{et}(T) \rangle = x_e + x_{se} \left[1 + \frac{m_{se} v_{se}^2}{k_B T_q} \right] \frac{m_e \nu_e}{m_{se} \nu_{se}}. \quad (62)$$

Thus, in a first approximation, the average enhancement per electron is significantly smaller than the enhancement per solectron (Fig. 7). Of most physical interest is the region around the maximum of enhancement. We ought

to insist that the results obtained above have to be considered as first qualitative estimates of the transport enhancement by solectron excitations. The most critical reason is that so far only approximate estimates of the free parameters of our theory

$$A, B, |E_{se}|, m_{se}, v_{se}, \omega_0, \omega_{se}, \nu_{se}$$

are known. Further work is needed to allow for more accurate values.

8 Discussion and conclusion

This work is devoted to soliton-assisted enhanced transport in thermal systems in the range of moderately high to low temperatures roughly around 10^2 K. We have shown that thermal solitons may be excited which may form with electrons bound states, called solectrons. These solectrons are able to move along crystallographic axes nearly without losses by scattering [21]. In this respect, soliton assisted transport is similar to ballistic transport [18]. At moderately high temperatures solectrons are rather stable and may provide a considerable enhancement of transport. The enhancement factor depends on the temperature, the soliton density, the fraction of solectrons and their lifetime. The probability of forming solectrons in the range $T \simeq 0.01-0.05D$ (where D is the depth of the Morse well) reaches a maximum and then goes down and also solectrons are not stable at too high temperatures.

We show that for appropriate parameter values and in the range of temperatures $T \simeq 0.01-0.1$ (in units $2D$), the enhancement may reach values around two orders of magnitude. We have shown that incorporating quantum effects is a must in order to locate its maximum.

Finally, let us explore the case of a fiber bundle of parallel oriented linear lattices of Morse atoms with only weak lateral interactions, assuming a total density of lattice points of about 10^{29} m^{-3} . This may roughly mimic a cubic crystal with one or two crystallographic axes, though this is a more complicated case. Better is to have in mind a stretched polyacetylene or other polymer material. Assuming that one third of the lattice points are doped with electrons and that about 30 percent of the possible number of solitons are excited, for a temperature around 10^2 K, the estimates for the solectron density and the contribution to electrical conductivity are, respectively,

$$n_{se} \simeq 10^{28} \text{ m}^{-3}; \quad \sigma_{se} \simeq 5 \times 10^7 \text{ S m}^{-1}. \quad (63)$$

Recall that typical metals have conductivities in the range $\sigma \simeq 10^5-10^8 \text{ S m}^{-1}$. Our solectron model shows that the electrical conductivity is in that range. Therefore we may consider soliton-assisted or, more appropriately, solectron-driven transport as a promising candidate, to say the least, for developing new materials with quite high conductivity (for stretched doped polyacetylene the value is $8 \times 10^6 \text{ S m}^{-1}$).

A complete kinetic theory of solectron-driven transport is yet to be developed. In particular, the formation

of bisolectrons and Bose-Einstein effects ought to be included. This is significant since many observations show that the essential contribution to charge transport in, e.g., conducting polymers comes from spinless particles [50] which in our case may correspond to adding bisolectron contributions [38] thus eventually improving upon the result (62).

This research was supported by the Spanish *Ministerio de Ciencia e Innovacion*, under Grant MAT2011-26221 and by the Ministry of Education and Science of the Russian Federation.

References

1. A. Heeger, S. Kivelson, J.R. Schrieffer, W.P. Su, *Rev. Mod. Phys.* **60**, 781 (1988)
2. A. Heeger, *Semiconducting and metallic polymers*, in *Nobel Lectures, Chemistry, 1996-2000*, edited by I. Grenthe (World Scientific, Singapore, 2003)
3. A.G. McDiarmid, *Ang. Chem. Int. Ed.* **40**, 2581 (2001)
4. W.P. Su, J.R. Schrieffer, A.J. Heeger, *Phys. Rev. Lett.* **42**, 1698 (1979)
5. T. Holstein, *Ann. Phys.* **8**, 325 (1959)
6. T. Holstein, *Ann. Phys.* **8**, 343 (1959)
7. A.S. Davydov, *Biology and Quantum Mechanics* (Pergamon, New York, 1982)
8. A.S. Davydov, *Solitons in Molecular Systems* (Reidel, Dordrecht, 1991)
9. A.S. Davydov, *Rep. Phys.* **40**, 408 (1979)
10. A.C. Scott, *Phys. Rev. A* **26**, 578 (1982)
11. A.C. Scott, *Phys. Rep.* **217**, 1 (1992)
12. A.S. Davydov, A.V. Zolotaryuk, *Phys. Scr.* **30**, 126 (1984)
13. A.V. Zolotaryuk, K.H. Spatschek, A.V. Savin, *Phys. Rev. B* **54**, 266 (1996)
14. *Davydov's Soliton Revisited. Self-trapping of Vibrational Energy in Protein*, edited by P.L. Christiansen, A.C. Scott (Plenum, New York, 1990)
15. L. Cruzeiro, *J. Phys. B* **41**, 195401 (2008)
16. E.G. Wilson, *J. Phys. C* **16**, 6739 (1983)
17. A.K. Geim, *Int. J. Mod. Phys. B* **25**, 4055 (2011)
18. X. Du, I. Skachko, A. Barker, E.Y. Andrei, *Nat. Nanotechnol.* **3**, 491 (2008)
19. K.A. Moler, *Nature* **468**, 643 (2010)
20. M.G. Velarde, W. Ebeling, A.P. Chetverikov, *C.R. Acad. Sci. (Paris)* **340**, 910 (2012)
21. A.P. Chetverikov, W. Ebeling, M.G. Velarde, *Contr. Plasma Phys.* **51**, 814 (2013)
22. W. Ebeling, A.P. Chetverikov, G. Röpke, M.G. Velarde, *Contr. Plasma Phys.* **53**, 736 (2013)
23. D. Hennig, M.G. Velarde, A.P. Chetverikov, W. Ebeling, *Phys. Rev. E* **76**, 046602 (2007)
24. M.G. Velarde, W. Ebeling, A.P. Chetverikov, *Int. J. Bifurc. Chaos* **18**, 3815 (2008)
25. O.G. Cantu-Ros, L. Cruzeiro, M.G. Velarde, W. Ebeling, *Eur. Phys. J. B* **80**, 545 (2011)
26. K.J. Donovan, E.G. Wilson, *Philos. Mag. B* **44**, 9 (1981)
27. K.J. Donovan, E.G. Wilson, *Philos. Mag. B* **44**, 31 (1981)
28. K.J. Donovan, P.D. Freeman, E.G. Wilson, *J. Phys. C* **18**, L275 (1985)
29. A.A. Gogolin, *Phys. Rep.* **157**, 347 (1988)

30. M. Kuwabara, Y. Ono, J. Phys. Soc. Jpn **63**, 1081 (1994)
31. M.G. Velarde, A.P. Chetverikov, W. Ebeling, E.G. Wilson, K.J. Donovan, Europhys. Lett. **106**, 27004 (2014)
32. M. Toda, *Nonlinear Waves and Solitons* (Kluwer, Dordrecht, 1983)
33. L.D. Landau, Phys. Z. Sowjetunion **3**, 664 (1993)
34. S.I. Pekar, *Untersuchungen über die Elektronentheorie* (Akademie Verlag, Berlin, 1954)
35. J.C. Slater, in *Quantum Theory of Molecules and Solids* (McGraw-Hill, New York, 1974), Vol. 4
36. P. Morse, Phys. Rev. **34**, 57 (1929)
37. G.B. Whitham, *Linear and Nonlinear Waves* (Wiley, New York, 1974)
38. L. Brizhik, A.P. Chetverikov, W. Ebeling, G. Röpke, M.G. Velarde, Phys. Rev. B **85**, 245105 (2012)
39. A.P. Chetverikov, W. Ebeling, G. Röpke, M.G. Velarde, Contr. Plasma Phys. **47**, 465 (2007)
40. V. Muto, A.C. Scott, P.L. Christiansen, Phys. Lett. A **136**, 33 (1981)
41. F. Marchesoni, C. Lucheroni, Phys. Rev. E **44**, 5303 (1991)
42. A.P. Chetverikov, W. Ebeling, G. Röpke, M.G. Velarde, Contr. Plasma Phys. **51**, 814 (2011)
43. A.P. Chetverikov, W. Ebeling, M.G. Velarde, Eur. Phys. J. B **80**, 137 (2011)
44. A.P. Chetverikov, W. Ebeling, M.G. Velarde, Eur. Phys. J. B **85**, 291 (2012)
45. R.P. Feynman, *Statistical Mechanics: A Set of Lectures*, (Benjamin, Reading, Massachusetts, 1972)
46. Yu.L. Klimontovich, *Statistical theory of open systems*, (Janus Moscow & Kluwer, Dordrecht, 1995)
47. T.L. Curtright, D.B. Fairlie, C.K. Zachos, *A concise treatise on quantum mechanics in phase space* (World Scientific, Singapore, 2014)
48. R. Balescu, *Equilibrium and nonequilibrium statistical mechanics* (Wiley, New York, 1975)
49. W. Ebeling, M.G. Velarde, A.P. Chetverikov, Proc. Conf. NDES-12; Proc. Conf. ICENET-12 (2012)
50. J.I. Bredas, G.B. Street, Acc. Chem. Res. Am. Chem. Soc. **18**, 308 (1985)